

## Spatial instabilities and dislocation-loop ordering in irradiated materials

Daniel Walgraef\* and Nasr M. Ghoniem

*Mechanical, Aerospace, and Nuclear Engineering Department, University of California, Los Angeles, Los Angeles, California 90024*

(Received 13 October 1988)

The formation of inhomogeneous distributions of vacancy loops in irradiated materials is discussed in the framework of a dynamical model based on the rate theory of radiation damage. Dislocation structures are associated with dynamical instabilities due to the competition between defect motion and interactions. The dependence of the critical wavelength of the microstructures on material variables, such as the displacement-damage rate, network-dislocation density, or temperature, is obtained. The postbifurcation analysis is performed in the weakly nonlinear regime, where the selection and stability properties of three-dimensional structures are investigated.

### I. INTRODUCTION

Irradiated materials and alloys present several types of spatial structures such as dislocation microstructures and void lattices.<sup>1</sup> These structures, which correspond to the spatial organization of defect populations, have a strong influence on the physical and mechanical properties of the materials. Hence an understanding of the formation, selection, and stability of defect patterns in irradiated materials is of primary importance from both practical and fundamental points of view. Several attempts have been made to describe these self-organization phenomena in the framework of kinetic models for defect populations. These models are based on rate equations describing the basic elements of the collective behavior of each defect population. These basic elements are described as (1) defect motion which is due to diffusion processes in the case of point defects such as vacancies and interstitials, or due to climb, glide, or cross slipping in the case of dislocations; (2) defect interactions corresponding to, for example, recombination of point defects, capture or emission of point defects by microstructures; and (3) defect-creation mechanisms induced by the effect of the external constraint which is the irradiation in the case discussed here.

Since the dynamics of point defects is much faster than that of larger microstructural features, and since the mobility of interstitials is much greater than that of vacancies, all the ingredients needed for the occurrence of pattern-forming instabilities are present in this type of description. Effectively, far-from-equilibrium systems where several species or fields with different mobilities interact via nonlinear couplings are known to be potentially able to display patterning phenomena on macroscopic space scales as extensively shown in a large number of hydrodynamical and other physicochemical systems.<sup>2</sup> Such instabilities have been investigated by several authors in the study of irradiated metals and alloys. In some cases, the critical wavelength of the microstructures has been determined as well.<sup>3,4</sup> However, questions related to the postbifurcation behavior of irradiated materials remain unanswered. It is of interest to investigate the geometry,

the symmetries, and the stability ranges of the selected structures. As indicated by Krishan,<sup>5</sup> the nature of the selection mechanisms and how the selected patterns are influenced by the underlying lattice symmetry, or by other materials and irradiation conditions, remain largely unexplored.

Up to now these aspects of radiation-induced microstructural ordering have not been theoretically addressed despite their practical interest, since current analyses are restricted to one-dimensional systems. The difficulties of the postbifurcation analysis lie in the fact that the complexity of the dynamics does not allow, in general, the attainment of analytic solutions for the various concentrations. However, near the instability or bifurcation points, the dynamics may be reduced to much simpler forms by taking advantage of the time- and space-scale separation between stable and unstable modes and by projecting the dynamics on its unstable manifold.<sup>6</sup> The resulting slow-mode dynamics which governs the system evolution on its longest time scale becomes similar to the time-dependent Landau-Ginzburg dynamics describing phase transitions in equilibrium systems. This description leads then to amplitude equations for the patterns and allows the derivation of their phase dynamics. Pattern selection and stability may then be discussed in this framework. These analyses have been shown to be of wider generality, relevant to the description of many experimental results in hydrodynamical, chemical, or biochemical systems. In this paper, it is our aim to analyze in this framework a simple model recently proposed by Murphy to describe the formation of spatially inhomogeneous distributions of vacancy loops in irradiated metals.<sup>4</sup> Furthermore, we develop relationships between the shape of the marginal-stability curve and simple physical properties of the system, perform postbifurcation analysis in the weakly nonlinear regime, and investigate the selection and stability properties of the emerging three-dimensional (3D) structures. The paper is organized as follows. In Sec. II we recall the kinetic model and its properties, while the linear stability analysis, the location of the first bifurcation, and the properties of marginal stability are discussed in Sec. III. The postbifurcation regime is analyzed

in Sec. IV, while Sec. V is devoted to a general discussion of the model in light of available experimental data.

## II. THE DYNAMICAL MODEL

The model proposed by Murphy<sup>4</sup> is based on the rate theory of radiation damage and describes the coupled dynamics of vacancies, interstitials, and vacancy loops. This model was originally developed by Bullough, Eyre, and Krishan,<sup>7</sup> and expanded later by Ghoniem and Kulcinski<sup>8</sup> to include the dynamics of point defects in the fully dynamic rate theory. The network dislocations which are also present in the material are assumed to have a constant uniform distribution and interstitial loops are neglected. The basic mechanisms which are taken into account correspond to (1) the diffusion of point defects (the diffusion coefficients will be considered as isotropic as a first step; anisotropies due to the crystal structure will also be incorporated at a later stage of the description), (2) the creation of point defects at a constant rate during irradiation (some of the vacancies are instantaneously trapped into vacancy loops by a cascade effect which is the dominant creation mechanism of these loops), and (3) the recombination of point defects, their migration to the loops and network dislocations, and the thermal emission of vacancies from loops and network dislocations.

Hence the kinetic equations for the defect concentrations are written as follows, where  $c_v$  corresponds to vacancies,  $c_i$  to interstitials, and where  $\rho_L$  and  $\rho_N$  are the line densities of vacancy loops and network dislocations:

$$\begin{aligned} \partial_t c_i &= K - \alpha c_i c_v + D_i \nabla^2 c_i - D_i c_i (Z_{iN} \rho_N + Z_{iL} \rho_L), \\ \partial_t c_v &= K(1 - \epsilon) - \alpha c_i c_v + D_v \nabla^2 c_v \\ &\quad - D_v [Z_{vN} (c_v - \bar{c}_{vN}) \rho_N + Z_{vL} (c_v - \bar{c}_{vL}) \rho_L], \\ \partial_t \rho_L &= \frac{1}{|\mathbf{b}| r_L^0} \{ \epsilon K - \rho_L [D_i Z_{iL} c_i - D_v Z_{vL} (c_v - \bar{c}_{vL})] \}, \end{aligned} \quad (1)$$

where  $K$  is the displacement-damage rate and  $\epsilon$  the cascade-collapse efficiency.  $D_i$  and  $D_v$  are the diffusion coefficients,  $\alpha$  is the recombination coefficient, and  $\mathbf{b}$

Burgers vector. The line density of vacancy loops,  $\rho_L$ , is given by  $\rho_L = 2\pi \bar{r}_L N_L$ , where  $\bar{r}_L$  and  $N_L$  are the average radius and the number density of the loops. The average loop radius is taken to be constant (with  $\bar{r}_L = r_L^0/2$ ,  $r_L^0/2$  being the initial radius of a vacancy loop).  $Z_{iL}$ ,  $Z_{iN}$ ,  $Z_{vL}$ , and  $Z_{vN}$  are the bias factors, and  $\bar{c}_{vN}$  and  $\bar{c}_{vL}$  are the thermally emitted vacancies from network dislocations and vacancy loops. The various coefficients appearing in these rate equations may be computed theoretically or related to measurable quantities, and for simplicity, the bias will be approximated by  $Z_{iL} = Z_{iN} = 1$  and  $Z_{vL} = Z_{vN} = 1 + B$  (the usual values for  $B$  being in the range 1–10%).<sup>7</sup>

## III. LINEAR-STABILITY ANALYSIS

In this section we develop a dimensionless form of the rate equations (1). A characteristic time scale is the time constant for vacancy diffusion to network dislocations. Upon using the following definitions:

$$\begin{aligned} \lambda_v &= D_v Z_{vN} \rho_N, \quad \bar{D}_{i(v)} = D_{i(v)} / \lambda_v, \quad \alpha / \lambda_v = \gamma, \\ P &= \gamma K / \lambda_v, \quad \tau = \lambda_v t, \end{aligned} \quad (2)$$

$$\mu = Z_{iN} D_i / Z_{vN} D_v = (1 + B) \frac{D_i}{D_v},$$

$$x = \frac{\rho_L}{\rho_N}, \quad x_i = \gamma c_i, \quad x_v = \gamma c_v, \quad \tau_0 = b r_L^0 \rho_N \gamma,$$

we obtain

$$\begin{aligned} \partial_\tau x_i &= P - \mu x_i (1 + x) - x_i x_v + \bar{D}_i \nabla^2 x_i, \\ \partial_\tau x_v &= P(1 - \epsilon) - (x_v - \bar{x}_{vN}) - x(x_v - \bar{x}_{vL}) \\ &\quad - x_i x_v + \bar{D}_v \nabla^2 x_v, \\ \tau_0 \partial_\tau x &= \epsilon P - x [\mu x_i - (x_v - \bar{x}_{vL})]. \end{aligned} \quad (3)$$

The linear-evolution matrix of inhomogeneous perturbations of the uniform steady state is given, in Fourier space, by

$$\begin{pmatrix} \omega + \mu(1 + x^0) + x_v^0 + q^2 \bar{D}_i & x_i^0 & \mu x_i^0 \\ x_v^0 & \omega + 1 + x^0 + x_i^0 + q^2 \bar{D}_v & x_v^0 - \bar{x}_{vL} \\ \mu x^0 & -x^0 & \omega + \Delta \end{pmatrix}, \quad (4)$$

where

$$\begin{aligned} \mu x_i^0 &= x_v^0 - \bar{x}_{vN}, \\ \epsilon P &= x^0 (\bar{x}_{vL} - \bar{x}_{vN}) = x^0 \Delta. \end{aligned} \quad (5)$$

It turns out that the characteristic equation has two negative roots while the third one may change its sign and becomes positive when

$$\begin{aligned} \mu A + q^2 \bar{D}_i \left[ A + 1 + B - \frac{\epsilon P}{\Delta^2} B (x_v^0 - \bar{x}_{vL}) \right] \\ + q^4 \bar{D}_i \bar{D}_v \leq 0, \end{aligned} \quad (6)$$

where

$$A = 1 + x_i^0 + \frac{x_v^0}{\mu} + \frac{\epsilon P}{\Delta}.$$

By taking the ratio of the bias versus the collapse efficiency as bifurcation parameter, the corresponding marginal-stability curve of this problem may be written as (by neglecting contributions of the order of  $x_i^0/x^0$ ,  $x_v^0/x^0$ ,  $\bar{x}_{vL}/x^0$ , and  $\bar{x}_{vN}/x^0$  which are vanishingly small in standard experimental situations),

$$\frac{B}{\epsilon} = \frac{1 + \frac{\Delta}{\epsilon P} (1 + q^2 \bar{D}_v) + \frac{1}{q^2 \bar{D}_v}}{1 - \frac{\epsilon (1 + q^2 \bar{D}_v)}{q^2 \bar{D}_v}} \quad (7)$$

and the critical point is defined by

$$\frac{B}{\epsilon} \Big|_c = \left[ 1 + \left( \frac{\Delta}{\epsilon P} \right)^{1/2} \right]^2 = \left[ 1 + \left( \frac{\rho_N}{\rho_L^0} \right)^{1/2} \right]^2 \quad (8)$$

with a critical wavelength given by

$$\lambda_c = 2\pi \left( \frac{\bar{D}_i \bar{D}_v}{\mu x^0} \right)^{1/4} \quad (9)$$

Hence, the uniform steady state may become unstable, when the dislocation bias overcomes the cascade-collapse efficiency, i.e.,

$$B > \epsilon \left[ 1 + \left( \frac{\rho_N}{\rho_L^0} \right)^{1/2} \right]^2,$$

or, at fixed bias, when the uniform loop density is sufficiently high, or the network density sufficiently low, i.e.,

$$\rho_L^0 > \frac{\rho_N}{(\sqrt{B/\epsilon} - 1)^2} \quad (10)$$

On expressing the critical wavelength in unscaled units,

$$\lambda_c = 2\pi \left[ \frac{D_v (\bar{c}_{vL} - \bar{c}_{vN})}{(1+B)\epsilon K \rho_N} \right]^{1/4},$$

we see that the wavelength decreases with increasing network-dislocation density, cascade-collapse efficiency, and damage rate. On the other hand, its temperature dependence is more difficult to assess since  $D_v$  is an increasing function of the temperature while  $(\bar{c}_{vL} - \bar{c}_{vN})$  is a decreasing function of the temperature, and its global behavior may vary from material to material. As an example, we consider the stainless steel (316SS) irradiated at 500°C with a displacement-damage rate of  $10^{-6}$  dpa  $s^{-1}$  (dpa is the displacement per atom).<sup>8</sup> The critical wavelength is nearly  $1.24 \mu\text{m}$  for solution-annealed material with a typical dislocation density of  $10^{13} \text{m}^{-2}$ . The wavelength is smaller for cold-worked material, on the order of  $0.39 \mu\text{m}$  for a dislocation density of  $10^{15} \text{m}^{-2}$ . The sensitivity of the critical wavelength to temperature variations is illustrated in Fig. 1, while Fig. 2 shows the effects of cascade-collapse efficiency  $\epsilon$  on the wavelength.

Furthermore, patterning phenomena should occur more readily when the network-dislocation density is small, and when cascade collapse is not important. From this analysis it turns out that beyond the critical point patterns could develop with wave numbers in the range

$$1 - (x^0)^{1/4} \left[ \frac{B}{\epsilon} - \frac{B}{\epsilon} \Big|_c \right] < \frac{q^2}{q_c^2} < 1 + (x^0)^{1/4} \left[ \frac{B}{\epsilon} - \frac{B}{\epsilon} \Big|_c \right].$$

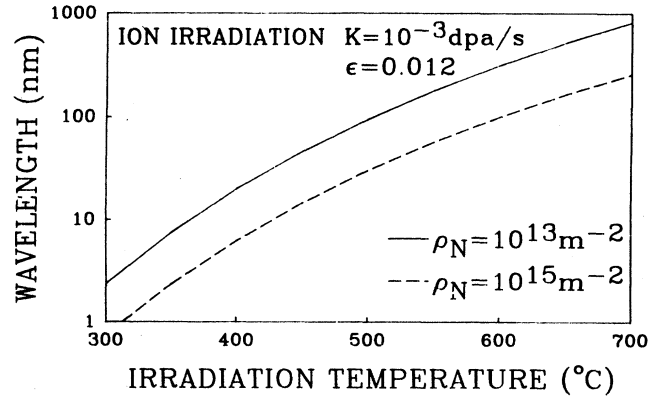


FIG. 1. Dependence of the critical wavelength on temperature for different values of the network-dislocation density.

However, the orientation and the number of wave vectors underlying the possible structures are not fixed, and the associated degeneracy may only be partly removed by a nonlinear analysis in the postbifurcation regime.

#### IV. THE AMPLITUDE EQUATIONS FOR THE MICROSTRUCTURES

The nonlinear character of the defect dynamics does not allow general analytical solutions for defect densities. However, near the instability points, it is possible to derive an approximate dynamic scheme able to reproduce the long-time evolution of the system. Effectively, around the bifurcation point, the dynamics is based on two types of modes: unstable ones and linearly stable ones which evolve on much shorter times scales. As a result, the stable modes are able to follow quasisteadily the evolution of the unstable ones and may be adiabatically eliminated.<sup>9</sup> The asymptotic behavior of the system is then described in terms of the unstable modes only. In fact, in the systems considered here, the fluctuations of vacancy and interstitial concentrations evolve much more

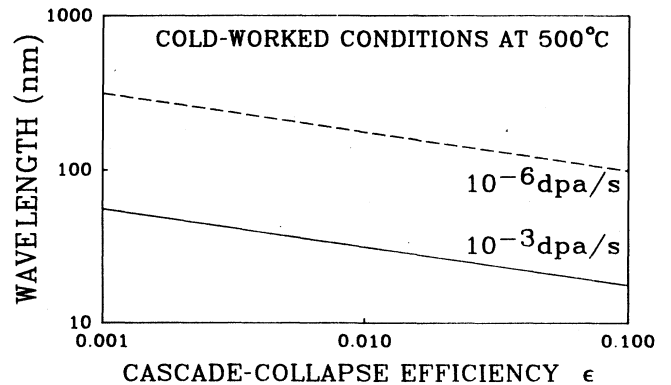


FIG. 2. Dependence of the critical wavelength on the cascade-collapse efficiency for different values of the displacement-damage rate.

rapidly than vacancy-loop-density fluctuations. Hence, the slow mode or order-parameter-like variable will be associated with the latter and on expanding the point-defect concentrations as a power series in the vacancy-loop density we obtain

$$\begin{aligned} x_q &= \rho_q + x^0, & x_{i,q} &= \rho_{i,q} + x_i^0 \\ x_{v,q} &= \rho_{v,q} + x_v^0, \\ \dot{\rho}_q &= -\frac{\Delta}{\tau_0} \rho_q - \frac{\epsilon P}{\Delta \tau_0} (\mu \rho_{i,q} - \rho_{v,q}) \\ &\quad - \frac{1}{\tau_0} \int dk \rho_{q-k} (\mu \rho_{i,k} - \rho_{v,k}) \end{aligned} \quad (11)$$

leading to

$$\begin{aligned} \dot{\rho}(\mathbf{x}, t) &= \left[ \frac{b-b_c}{b_c} - \xi_0^2 (q_c^2 + \nabla^2)^2 \right] \rho(\mathbf{x}, t) \\ &\quad + v \rho^2(\mathbf{x}, t) - u \rho^3(\mathbf{x}, t), \end{aligned} \quad (12)$$

where

$$b = B/\epsilon, \quad \xi_0^2 \propto (x_0)^{-1/2}, \quad v = 2/(x_0)^{3/2},$$

and  $u = 2/(x_0)^{5/2}$ .

It is known that, for  $b > b_c$ , the stable solutions of this Landau-Ginzburg type of dynamics correspond to<sup>10</sup> the following.

(1) Roll or wall structures associated with spatial modulations of the order parameter (here the vacancy-loop density) in one direction. They appear via a second-order-like transition, or supercritical bifurcation, and the amplitude equation for a structure of this type with wave vector  $\mathbf{q} = q_c \mathbf{1}_x$  may be written as follows:

$$\tau \dot{A} = \left[ \frac{b-b_c}{b_c} + \frac{4\xi_0^2}{q_c^2} (\nabla_x - \frac{i}{2q_c} \nabla_1^2)^2 \right] A - 3u |A|^2 A, \quad (13)$$

where  $\nabla_1^2 = \nabla_y^2 + \nabla_z^2$ .  $A(x, t)$  is the slowly varying amplitude of the structure defined by

$$\rho(\mathbf{x}, t) = A(\mathbf{x}, t) e^{iq_c x} + A^*(\mathbf{x}, t) e^{-iq_c x}.$$

The steady-state amplitude of a wall structure of critical wavelength is then given by  $|A| = \sqrt{(b-b_c)/3ub_c}$ .

(2) Rodlike hexagonal or triangular structures appearing via first-order-like transition or subcritical bifurcations, defined by the following amplitude equations:

$$\begin{aligned} \rho(\mathbf{x}, t) &= \sum_{i=1}^3 A_i(\mathbf{x}, t) e^{iq_i \cdot \mathbf{x}} + \text{c.c.}, \\ |\mathbf{q}_i| &= q_c, \quad \mathbf{q}_1 + \mathbf{q}_2 + \mathbf{q}_3 = 0, \\ \tau \dot{A}_i &= \left[ \frac{b-b_c}{b_c} + \frac{4\xi_0^2}{q_c^2} (\mathbf{q}_i \cdot \nabla)^2 \right] A_i + v A_{i-1}^* A_{i+1}^* \\ &\quad - 3u \left[ |A_i|^2 + 2 \sum_{j \neq i} |A_j|^2 \right] A_i. \end{aligned} \quad (14)$$

The steady state is given by ( $|A_i| = A$ )

$$\frac{b-b_c}{b_c} A + v A^2 - 15u A^3 = 0.$$

(3) bcc lattices or filamental structures of cubic symmetry, also associated with a subcritical bifurcation and defined similarly to hexagonal structures but with six pairs of wave vectors. The corresponding steady state is then given by

$$\begin{aligned} \rho(\mathbf{x}) &= A \left[ \cos \frac{q_c}{\sqrt{2}} x \cos \frac{q_c}{\sqrt{2}} y + \frac{\cos q_c}{\sqrt{2}} y \cos \frac{q_c}{\sqrt{2}} z \right. \\ &\quad \left. + \cos \frac{q_c}{\sqrt{2}} z \cos \frac{q_c}{\sqrt{2}} x \right] \end{aligned}$$

with

$$\frac{b-b_c}{b_c} A = 2v A^2 - 33u A^3 = 0. \quad (15)$$

When the bifurcation parameter is increased, the 2d and 3d structures may in turn become unstable [the hexagonal structure for  $(b-b_c)/b_c > 4v^2/3u$  and the bcc structure for  $(b-b_c)/b_c > 3v^2/u$ ]. The corresponding phase diagram for bcc and planar walls is displayed in Fig. 3.

Hence, between threshold and  $3v^2/u$ , bcc dislocation structures should be expected, while above this limit the structure should consist of regularly spaced planes of maximum density. Since  $v^2/u = (D_v \Delta \rho_N / \epsilon K)^{1/2}$ , the bcc domain is expected to increase either with temperatures below 1000 °C and with network dislocation densities. In the example of 316L steel cited above, the reduced distance above threshold,  $(b-b_c)/b_c$ , is of the order of 2, for a bias factor of 0.035 and a cascade-collapse efficiency of 0.012. At irradiation temperatures of 500 °C, and for a displacement-damage rate of  $10^{-6}$  dpa s<sup>-1</sup>, the bcc stability limit is about 3.8 for a network dislocation density of  $10^{14}$  m<sup>-2</sup> and nearly equal to 1.2 for  $\rho_N = 10^{13}$  m<sup>-2</sup>. In

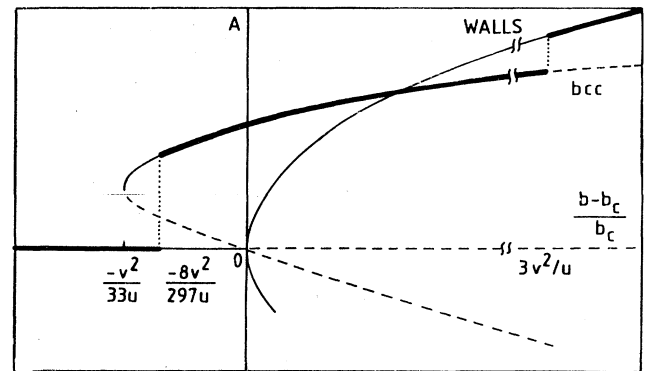


FIG. 3. Schematic bifurcation diagram associated with the amplitude equation for the microstructures showing the transition from bcc to wall structures (solid lines represent stable states, dashed lines represent unstable states, and heavy lines correspond to the minimum of the associated Lyapunov functional).

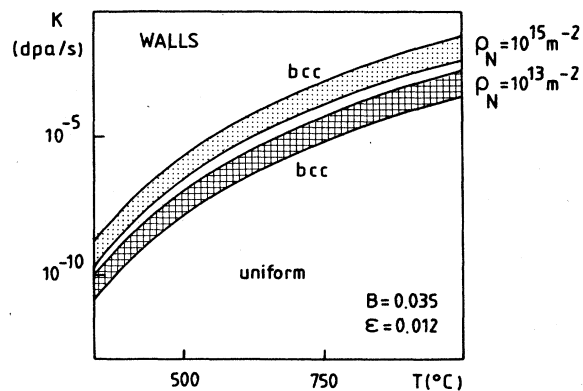


FIG. 4. Stability domains of bcc and planar structures versus displacement damage rate and temperature for different values of the network-dislocation density.

fact, under these conditions, a transition between bcc structures and planar walls should occur for network dislocation densities around  $2.77 \times 10^{12} \text{ m}^{-2}$ , the bcc structure being selected for higher densities and the planar structures for lower densities. The stability domains of bcc and planar structures versus network-dislocation density, displacement-damage rate, or temperature is displayed in Fig. 4.

In the case of an anisotropic diffusion of interstitials as in hcp materials, where the mobility of interstitials is much larger in the basal planes than between these planes, it is easy to show with the same method, that the stable patterns for vacancy loops correspond to planar arrays with planes of maximum density parallel to the planes of high-interstitial mobility in agreement with experimental observations.<sup>11</sup>

The result of the present analysis obtained in the weakly nonlinear regime beyond the pattern forming instability should, of course, be confronted to detailed experimental investigations and to at least 2D numerical simulations. It is interesting to note that recent experimental observations by Jäger<sup>12</sup> indicate that spatial microstructure modulation is a general phenomenon under ion-irradiation conditions where cascade are produced. Over a limited range of conditions, Jäger observed that the wavelength was insensitive to temperature, dose rate, and type of primary knock-on atom. Dislocation loops and tangles were found to be arranged in planar arrangements (walls), with a wavelength of  $0.03\text{--}0.06 \mu\text{m}$ . While the model discussed here is in general agreement with these experimental observations, it should be viewed as a step toward a generalized theoretical explanation of the nature of microstructure ordering under irradiation.

## V. DISCUSSION

The occurrence of pattern-forming instabilities seems natural for defect populations in irradiated metals and alloys. It mainly results from the different mobilities and bias in the migration of point defects to line defects such as vacancy loops or network dislocations. We showed

here that structures with different symmetries may be simultaneously stable beyond the primary bifurcation. For example, when the diffusion and interactions of point defects are isotropic, the maxima of the vacancy loop density may either correspond to bcc lattices or planar arrays. Hence, these structures could be in nonparallel orientations, i.e., with a structure different from the structure of the host lattice. On increasing further the displacement-damage rate, bcc lattices become unstable, and a first-order-like transition should occur to planar structures. In the case of anisotropic interstitial diffusion, planar structures should be the rule. Hence, since the symmetry of the defect structures is a crucial issue in irradiated material,<sup>13</sup> the present analysis shows that a careful study of the postbifurcation regime is needed to test the relevance of particular kinetic models to the interpretation of experimental observations.

Before we conclude this paper, it is important to discuss available experimental results and how they relate to the current model. A number of experimental observations have been made on the ordering of the dislocation-loop microstructure under irradiation. Hulett *et al.*<sup>14</sup> found walls containing clusters of dislocations and dislocation loops about  $10 \mu\text{m}$  wide located parallel to the (111) planes in high-purity-copper neutron irradiated at about  $400^\circ\text{C}$ . The clusters were separated by strained, but defect-free regions about  $100 \mu\text{m}$  wide. Their specimens were well-annealed copper single-crystal wafers, having dislocation densities varying between  $10^7$  and  $10^8 \text{ m}^{-2}$ . This experiment shows that for very low dislocation densities and low damage rates, the wavelength can be very large. On a much finer scale, Kulcinski and Brimhall<sup>15</sup> found an ordered cubic lattice of loops and stacking fault tetrahedra running along  $\langle 100 \rangle$  directions in nickel ion bombarded at  $280\text{--}450^\circ\text{C}$ . Also, Sprague and Smidt<sup>16</sup> found similar rows of loops in nickel ion bombarded at  $350$  and  $400^\circ\text{C}$ , but did not detect 3D order to the arrangement. The reported wavelengths for the ion-irradiated cases of samples containing high-dislocation densities are generally of the order of  $0.03\text{--}0.05 \mu\text{m}$ . Planar arrays of loops have already been observed in a number of noncubic materials such as U (Ref. 17), BeO (Ref. 18), Ti (Ref. 19), Mg (Ref. 20), and Zr (Ref. 21). Stiegler and Farrell<sup>22</sup> found 3D arrays of loops in neutron-irradiated nickel and aluminum in the presence of voids. In their experiments, alignment of loops occurred in nickel specimens irradiated to fluences of about 1 dpa. The loops were arranged on a cubic lattice with loop-free isles separating loop clusters about  $0.03 \mu\text{m}$  across.

Even though some of these experimental observations on loops date back to the early 1960's, no physical model was proposed to explain the dependence of the wavelength or the merging structure on irradiation and material variables. Our current model seems to provide a simple explanation for the dependence of the wavelength on the displacement-damage rate, network-dislocation density, and on temperature. A joint, systematic, experimental, and theoretical effort may provide a complete understanding of microstructure ordering in irradiated alloys.

## ACKNOWLEDGMENTS

We would like to acknowledge the support of the U.S. Department of Energy, Office of Fusion Energy, for this

research. Financial assistance through DOE Grant No. DE-FGO3-84ER52110 with UCLA is greatly appreciated. D. W. acknowledges financial support also from the National Fund for Scientific Research (Belgium).

- 
- \*Permanent address: Faculté des Sciences, Université Libre de Bruxelles, CP 231, Brussels, Belgium.
- <sup>1</sup>*Nonlinear Phenomena in Materials Science*, edited by G. Martin and L. P. Kubin (Transtech, Aedermannsdorf, Switzerland, 1988).
- <sup>2</sup>G. Nicolis and I. Prigogine, *Self-Organization in Nonequilibrium Systems* (Wiley, New York, 1977).
- <sup>3</sup>G. Martin, *Phys. Rev. B* **30**, 1424 (1984).
- <sup>4</sup>S. M. Murphy, *Europhys. Lett.* **3**, 1267 (1987).
- <sup>5</sup>K. Krishan, *Radiat. Eff.* **66**, 121 (1982).
- <sup>6</sup>J. Guckenheimer, J. Moser, and S. Newhouse, *Dynamical Systems* (Birkhauser, Boston, 1980).
- <sup>7</sup>R. Bullough, B. L. Eyre, and K. Krishan, *J. Nucl. Mat.* **44**, 121 (1975).
- <sup>8</sup>N. M. Ghoniem and G. L. Kulcinski, *Radiat. Eff.* **39**, 47 (1978).
- <sup>9</sup>H. Haken, *Z. Phys. B* **21**, 105 (1975).
- <sup>10</sup>D. Walgraef, G. Dewel, and P. Borckmans, *Adv. Chem. Phys.* **49**, 311 (1982).
- <sup>11</sup>J. H. Evans, *Mater. Sci. Forum* **15-18**, 869 (1987).
- <sup>12</sup>W. Jäger, P. Ehrhart, and W. Schilling, in *Nonlinear Phenomena in Materials Science*, edited by G. Martin and L. P. Kubin (Transtech, Aedermannsdorf, Switzerland, 1988), p. 279.
- <sup>13</sup>R. W. Cahn, *Nature* **329**, 284 (1987).
- <sup>14</sup>L. D. Julett, Jr., T. O. Baldwin, J. C. Crump III, and F. W. Young, *J. Appl. Phys.* **39**, 3945 (1968).
- <sup>15</sup>G. L. Kulcinski and J. L. Brimhall, in American Society for Testing and Materials Report No. ASTM-STP 529, 1973, p. 258.
- <sup>16</sup>J. A. Sprague and F. A. Smidt, Jr. (unpublished).
- <sup>17</sup>B. Hudson, *Philos. Mag.* **10**, 949 (1964).
- <sup>18</sup>J. Wilks and F. J. P. Clarke, *J. Nucl. Mater.* **14**, 179 (1964).
- <sup>19</sup>J. L. Brimhall, G. L. Kulcinski, H. E. Kissinger, and B. Mastel, *Radiat. Eff.* **9**, 273 (1971).
- <sup>20</sup>A. Jostons and K. Farrel, *Radiat. Eff.* **15**, 217 (1972).
- <sup>21</sup>E. F. Koch and D. Lee, *Proceedings of the 31st Annual EMSA Meeting* (Clartor, Baton Rouge, 1973), p. 88.
- <sup>22</sup>J. O. Steigler and K. Farrell, *Scr. Metall.* **8**, 651 (1974).